

# Robust PID controller design for rigid uncertain spacecraft using Kharitonov theorem and vectored particle swarm optimization

Supanna S. Kumar<sup>1\*</sup>, C. Shreesha<sup>2</sup>, N.K. Philip<sup>3</sup>

<sup>1</sup>Department of Electrical and Electronics Engineering, N.M.A.M Institute of Technology, Nitte, India.

<sup>2</sup>Department of Instrumentation and Control Engineering, Manipal Institute of Technology, Manipal University, Manipal, India.

<sup>3</sup>Control Dynamics and Simulation Group, ISRO Satellite Centre, ISRO, Bengaluru, India.

## Abstract

This paper presents a robust Proportional Integral Derivative controller design methodology for three axis attitude control of a rigid spacecraft with parametric uncertainty using a combination of Kharitonov theorem and vectored particle swarm optimization based approaches. A controller is designed for each of the three axes using a systematic graphical approach. Here, a plot of the stability boundary loci in the integral gain versus proportional gain parameter plane, for the specified gain and phase margins for each of the Kharitonov interval plants is used to determine the region representing the set of all PID controllers that satisfy the desired performance and stability requirements. Vectored particle swarm optimization technique is used to determine the optimized proportional and integral gain values. The spacecraft attitude control system is simulated using Matlab-Simulink tool which shows that the designed controller provides stability, robustness, good reference pointing and disturbance rejection for perturbations within the specific bounds.

**Keywords:** Attitude control, kharitonov theorem, rigid spacecraft, robust optimization, uncertain system.

## 1. Introduction

The attitude and orbit specifications of satellites are very stringent. Since satellites are subjected to a number of external disturbances, the designed attitude controller must be able to meet the stability and performance requirements in view of varying parameters of the attitude control system. The use of classical control theory based design approach [1] is not amenable in case of uncertain systems since stability tests cannot be carried out on all the systems representing the family of transfer functions of the perturbed system. Also, Proportional-Integral-Derivative (PID) control is still the most desired type of control in industries because of its ease of implementation. This has resulted in the use of an approach based on Kharitonov theorem for designing robust PI/PID controllers for interval uncertain systems [2], [3], [4], [5], [6].

The spacecraft is modeled as a rigid body [7], with parameters varying within an interval. Techniques such as sliding mode control [8], [9],[10],[11],[12], [13], [14], integral with full state feedback control [15], feedback linearization [16], linear quadratic regulator control [17] and adaptive control [18], [19], [20] have been used to design robust controllers for rigid spacecraft systems. Attitude control of rigid body spacecrafts where the control torque output from the actuator experiences saturation has been described [21]. A robust PID controller using sliding mode approach for attitude control of spacecrafts subject to constraints on control torque and velocity has been demonstrated [22]. Unlike some of the techniques mentioned above, the Kharitonov based approach adopted in the work presented here is not a trial and error method but involves a systematic procedure which results in a robust controller with good noise rejection and desired performance.

Based on Kharitonov theorem, we define a set of Kharitonov interval plants which are obtained using the minimum and

maximum values of the interval polynomial coefficients of the transfer functions of the uncertain interval plant. For each of the Kharitonov interval plants, a stability boundary locus is plotted in the integral gain ( $K_i$ ) versus proportional gain ( $K_p$ ) parameter plane, keeping derivative gain ( $K_d$ ) fixed, for the phase and gain margin bounds chosen. The resulting overlapping region contains all the controller parameter sets which guarantee the imposed gain and phase margin bounds besides stability as proposed by Huang and Wang [23]. This controller parameter set satisfies only the phase margin and gain margin specifications. The use of particle swarm optimization (PSO) [24] allows us to choose the best  $K_p$  and  $K_i$  gains that results in an optimum performance in terms of peak overshoot, rise time, settling time and steady state error from among the obtained controller parameter set. The PSO technique has been applied to obtain optimized PID controllers by many researchers [25], [26], [27]. Standard PSO techniques are time consuming which can become a limiting factor when the system is to be implemented. The vectored particle swarm optimization (VPSO) technique overcomes this limitation since it makes use of vectors which improves the optimization time significantly [28]. Hence, from the intersecting region, an optimized PID controller is obtained using vectored particle swarm optimization so as to minimize the fitness function.

In case of uncertain interval systems, tuning the PID controller gains becomes challenging since it involves trial and error method and hence achieving the required performance within a given time frame may not be guaranteed. The Kharitonov based controller design method follows a systematic procedure and the use of vectored PSO gives fast results making the proposed technique advantageous.

Three PID controllers designed are used to simulate three axis attitude control of the spacecraft using Matlab-Simulink tool.

## 2. Controller design methodology

A PID controller has been designed for each of the three axes. The controller is such that the proportional and integral components work on the error signal and the derivative component works on the actual attitude angle resulting in a two degree of freedom PID controller. Such a controller is chosen since it can achieve a good set point tracking as well as fast disturbance rejection. The spacecraft inertia and actuator gain and time constant are considered as uncertain parameters which vary within specific bounds.

From Euler's moment equation, the external torque is given by,

$$T = \dot{h} = J\dot{\omega} = J\ddot{\theta} \quad (1)$$

where  $h$  is the angular momentum in N-m-s,  $\omega$  is the angular velocity in rad/s,  $\theta$  is the attitude angle in radians and  $J$  is the spacecraft moment of inertia about an axis in kg-m<sup>2</sup>.

The transfer function of the rigid spacecraft is given by,

$$\frac{\theta(s)}{T(s)} = \frac{1}{Js^2} \quad (2)$$

### Initial design of PD parameters

To account for the effect of limitation on the control torque output, a torque saturation block is considered at the input of the spacecraft block as in Fig. 1.

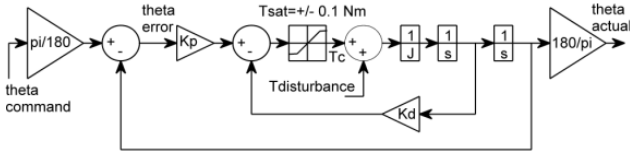


Fig.1: Closed loop attitude control with PD controller

From Fig. 1,

$$\frac{T_{c\max}}{\theta_{e\max}} = K_p \quad (3)$$

where  $T_{c\max}$  = maximum value of the control torque in N-m and

$\theta_{e\max}$  = maximum value of the attitude angle error in radians.

Assuming a maximum attitude error of about 5 degrees and maximum control torque output of 0.1 N-m we have,

$$K_p = \frac{0.1 \text{ N-m}}{5 \times \frac{\pi}{180} \text{ rad}} \approx 1 \quad (4)$$

Let,

$$K_p = 1 \quad (5)$$

The transfer function of the system shown in Fig. 1 is given by,

$$T(s) = \frac{\left(\frac{K_p}{J}\right)}{s^2 + \left(\frac{K_d}{J}\right)s + \left(\frac{K_p}{J}\right)} \quad (6)$$

Comparing Eq. 6 with the general form of the closed loop second order transfer function,

$$\omega_n^2 = \frac{K_p}{J} \quad (7)$$

$$2\xi\omega_n = \frac{K_d}{J} \quad (8)$$

where  $\omega_n$  = natural frequency of oscillation in rad/s and  $\xi$  = damping coefficient.

Using Eq. 5 and the given value of  $J$  about a particular axis in Eq. 7,  $\omega_n$  is calculated. Taking suitable value for  $\xi$ ,  $K_d$  is calculated using Eq. 8. Let a small integral parameter be introduced into the system to improve the steady state error. Let an actuator with transfer function  $K_a/(1+T_a s)$  be introduced into the system as in Fig. 2.

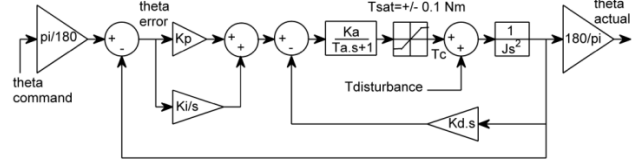


Fig. 2: Closed loop attitude control with PID controller

Next the effect of system parameter uncertainties is considered and a PID controller is designed for the same. The spacecraft moment of inertia  $J$  in kg-m<sup>2</sup>, actuator gain  $K_a$  and actuator time constant  $T_a$  in seconds are taken as the uncertain parameters which vary within specific intervals given by,

$$J \in [J^-, J^+], K_a \in [K_a^-, K_a^+], T_a \in [T_a^-, T_a^+] \quad (9)$$

Considering the effect of uncertainty, let the transfer function of the part of the circuit with actuator, spacecraft and  $K_d$  shown in Fig. 2 be given by,

$$G(s) = \frac{K_a}{JT_a s^3 + Js^2 + K_a K_d s} = \frac{a_0}{b_3 s^3 + b_2 s^2 + b_1 s} \quad (10)$$

where  $a_0 = K_a$ ,  $b_3 = JT_a$ ,  $b_2 = J$ ,  $b_1 = K_a K_d$ . The uncertain coefficients are given by,

$$a_0 \in [a_0^-, a_0^+], b_3 \in [b_3^-, b_3^+], b_2 \in [b_2^-, b_2^+], b_1 \in [b_1^-, b_1^+] \quad (11)$$

Using Kharitonov theorem, the uncertain system given by Eq. 10 can be represented by a family of eight Kharitonov plants  $G_{11}$  to  $G_{24}$  with the coefficient values as shown in Table 1 [6].

Table 1: Coefficients for the Kharitonov Plants

Plant	Coefficients			
	$a_0$	$b_3$	$b_2$	$b_1$
$G_{11}$	$a_0^-$	$b_3^+$	$b_2^+$	$b_1^-$
$G_{12}$	$a_0^-$	$b_3^-$	$b_2^+$	$b_1^+$
$G_{13}$	$a_0^-$	$b_3^+$	$b_2^-$	$b_1^-$
$G_{14}$	$a_0^-$	$b_3^-$	$b_2^-$	$b_1^+$
$G_{21}$	$a_0^+$	$b_3^+$	$b_2^+$	$b_1^-$
$G_{22}$	$a_0^+$	$b_3^-$	$b_2^+$	$b_1^+$
$G_{23}$	$a_0^+$	$b_3^+$	$b_2^-$	$b_1^-$
$G_{24}$	$a_0^+$	$b_3^-$	$b_2^-$	$b_1^+$

### Tuning the PI controller gains

In order to achieve the specified performance criteria of the uncertain system, we use a technique based on Kharitonov theorem as proposed by Huang and Wang [23]. Here, suitable gain and phase margins are chosen and for a fixed value of  $K_d$  assumed, stability boundary loci are plotted in the  $K_p$ - $K_i$  parameter plane. Then, from the intersecting stable region, optimized values of  $K_p$  and  $K_i$  are determined using vectored particle swarm optimization. The goal of optimization is to minimize the peak overshoot, settling time and steady state error.

Similarly, PID controllers are designed for the other two axes also.

## 3. Controller design for rigid spacecraft

The moment of inertia of the spacecraft about the roll, pitch and yaw axes are given by,

$$J_{0x} = 1150 \text{ kg-m}^2, J_{0y} = 1490 \text{ kg-m}^2, J_{0z} = 810 \text{ kg-m}^2 \quad (12)$$

According to Eq. 5,  $K_p = 1$ . Let the assumed integral gain before tuning the controller be given by,

$$K_i = 0.005 \text{ N-m/rad/s} \quad (13)$$

The calculated values of the derivative gains are,

$$K_{dx} = 47.95 \text{ N-m-s / rad}, K_{dy} = 54.58 \text{ N-m-s / rad}, K_{dz} = 40.24 \text{ N-m-s / rad} \quad (14)$$

We consider the moment of inertias to have an uncertainty of  $\pm 10\%$ . Let the actuator gain and time constant varying within their respective intervals be,

$$K_a \in [2, 2.2], T_a \in [0.5, 0.6] \text{ s} \quad (15)$$

As per specifications, the maximum allowable peak value is 20% and the maximum value of damping coefficient is 0.707. The  $a_0 \in [2, 2.2]$ ,  $b_3 \in [517.5, 759]$ ,  $b_2 \in [1035, 1265]$ ,  $b_1 \in [95.9, 105.49]$

The numerator and denominator Kharitonov polynomials for the transfer function in Eq. 10 are,

$$N_1(s) = 2, N_2(s) = 2.2, D_1(s) = 759s^3 + 1265s^2 + 95.9s, D_2(s) = 517.5s^3 + 1265s^2 + 105.49s, \quad (17)$$

$$D_3(s) = 759s^3 + 1035s^2 + 95.9s, D_4(s) = 517.5s^3 + 1035s^2 + 105.49s$$

Taking into account, all possible combinations of the Kharitonov polynomials in Eq. 17, the family of eight Kharitonov plants are obtained as,

$$G_{11}(s) = \frac{N_1(s)}{D_1(s)}, G_{12}(s) = \frac{N_1(s)}{D_2(s)}, G_{13}(s) = \frac{N_1(s)}{D_3(s)}, G_{14}(s) = \frac{N_1(s)}{D_4(s)}, \quad (18)$$

$$G_{21}(s) = \frac{N_2(s)}{D_1(s)}, G_{22}(s) = \frac{N_2(s)}{D_2(s)}, G_{23}(s) = \frac{N_2(s)}{D_3(s)}, G_{24}(s) = \frac{N_2(s)}{D_4(s)}$$

After the insertion of the gain and phase margin tester  $Ae^{j\theta}$  [23], in the system shown in Fig. 2, the characteristic polynomial becomes,

$$p(s) = \text{Numerator of} \left[ 1 + \left( K_p + \frac{K_i}{s} \right) \cdot A e^{-j\theta} \cdot G(s) \right] \quad (19)$$

Using Eq. 10 in Eq. 19 and replacing  $s$  with  $j\omega$ , the characteristic polynomial is given by.

$$a_0 \omega A \sin \theta = B_1, \quad a_0 A \cos \theta = B_2, \quad a_0 A \cos \theta = C_1, \quad (20)$$

$$-a_0 A \sin \theta = C_2, \quad b_3 \omega^4 - b_1 \omega^2 = D_1, \quad -b_2 \omega^3 = D_2$$

Using Eq. 21 in Eq. 20 and equating the real parts and imaginary parts to zero, we get,

$$K_p = \frac{C_1 D_2 - C_2 D_1}{B_1 C_2 - B_2 C_1} \quad (22)$$

$$K_i = \frac{D_1 B_2 - D_2 B_1}{B_1 C_2 - B_2 C_1} \quad (23)$$

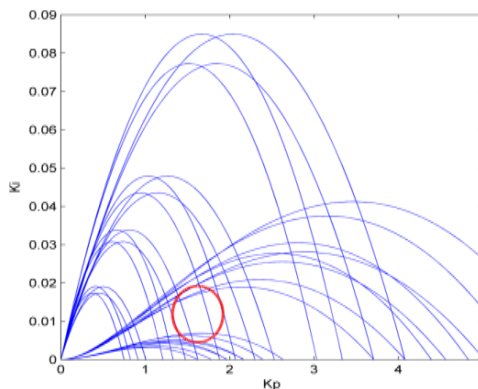


Fig. 3: Intersecting kharitonov region with specified gain and phase margins

Next, the optimum  $K_p$  and  $K_i$  values are obtained from within this region using vectored particle swarm optimization technique. The fitness function FF used is,

$$FF = (M_p + E_{ss})(1 - e^{-\beta}) + (T_s - T_r)e^{-\beta} \quad (24)$$

where  $M_p$  = peak overshoot,  $E_{ss}$  = steady state error,  $\beta$  = scaling factor,  $T_s$  = settling time in seconds,  $T_r$  = rise time in seconds.

corresponding phase margin bounds are calculated to be 48.15 degrees and 65.5 degrees. The minimum and maximum gain margin bounds are chosen to be 30 decibels and 38 decibels respectively.

For the roll axis, the coefficients of the transfer function in Eq. 10 are,

$$p(j\omega) = K_p a_0 \omega A \sin \theta + j K_p a_0 \omega A \cos \theta \quad (16)$$

$$+ K_i a_0 A \cos \theta - j K_i a_0 A \sin \theta + b_3 \omega^4 - b_1 \omega^2 - j b_2 \omega^3 \quad (17)$$

$$+ K_i a_0 A \cos \theta - j K_i a_0 A \sin \theta + b_3 \omega^4 - b_1 \omega^2 - j b_2 \omega^3 \quad (18)$$

$$+ K_i a_0 A \cos \theta - j K_i a_0 A \sin \theta + b_3 \omega^4 - b_1 \omega^2 - j b_2 \omega^3 \quad (19)$$

$$+ K_i a_0 A \cos \theta - j K_i a_0 A \sin \theta + b_3 \omega^4 - b_1 \omega^2 - j b_2 \omega^3 \quad (20)$$

$$+ K_i a_0 A \cos \theta - j K_i a_0 A \sin \theta + b_3 \omega^4 - b_1 \omega^2 - j b_2 \omega^3 \quad (21)$$

$$+ K_i a_0 A \cos \theta - j K_i a_0 A \sin \theta + b_3 \omega^4 - b_1 \omega^2 - j b_2 \omega^3 \quad (22)$$

$$+ K_i a_0 A \cos \theta - j K_i a_0 A \sin \theta + b_3 \omega^4 - b_1 \omega^2 - j b_2 \omega^3 \quad (23)$$

$$+ K_i a_0 A \cos \theta - j K_i a_0 A \sin \theta + b_3 \omega^4 - b_1 \omega^2 - j b_2 \omega^3 \quad (24)$$

$$+ K_i a_0 A \cos \theta - j K_i a_0 A \sin \theta + b_3 \omega^4 - b_1 \omega^2 - j b_2 \omega^3 \quad (25)$$

$$+ K_i a_0 A \cos \theta - j K_i a_0 A \sin \theta + b_3 \omega^4 - b_1 \omega^2 - j b_2 \omega^3 \quad (26)$$

$$+ K_i a_0 A \cos \theta - j K_i a_0 A \sin \theta + b_3 \omega^4 - b_1 \omega^2 - j b_2 \omega^3 \quad (27)$$

$$+ K_i a_0 A \cos \theta - j K_i a_0 A \sin \theta + b_3 \omega^4 - b_1 \omega^2 - j b_2 \omega^3 \quad (28)$$

$$+ K_i a_0 A \cos \theta - j K_i a_0 A \sin \theta + b_3 \omega^4 - b_1 \omega^2 - j b_2 \omega^3 \quad (29)$$

$$+ K_i a_0 A \cos \theta - j K_i a_0 A \sin \theta + b_3 \omega^4 - b_1 \omega^2 - j b_2 \omega^3 \quad (30)$$

$$+ K_i a_0 A \cos \theta - j K_i a_0 A \sin \theta + b_3 \omega^4 - b_1 \omega^2 - j b_2 \omega^3 \quad (31)$$

$$+ K_i a_0 A \cos \theta - j K_i a_0 A \sin \theta + b_3 \omega^4 - b_1 \omega^2 - j b_2 \omega^3 \quad (32)$$

$$+ K_i a_0 A \cos \theta - j K_i a_0 A \sin \theta + b_3 \omega^4 - b_1 \omega^2 - j b_2 \omega^3 \quad (33)$$

$$+ K_i a_0 A \cos \theta - j K_i a_0 A \sin \theta + b_3 \omega^4 - b_1 \omega^2 - j b_2 \omega^3 \quad (34)$$

$$+ K_i a_0 A \cos \theta - j K_i a_0 A \sin \theta + b_3 \omega^4 - b_1 \omega^2 - j b_2 \omega^3 \quad (35)$$

$$+ K_i a_0 A \cos \theta - j K_i a_0 A \sin \theta + b_3 \omega^4 - b_1 \omega^2 - j b_2 \omega^3 \quad (36)$$

$$+ K_i a_0 A \cos \theta - j K_i a_0 A \sin \theta + b_3 \omega^4 - b_1 \omega^2 - j b_2 \omega^3 \quad (37)$$

$$+ K_i a_0 A \cos \theta - j K_i a_0 A \sin \theta + b_3 \omega^4 - b_1 \omega^2 - j b_2 \omega^3 \quad (38)$$

$$+ K_i a_0 A \cos \theta - j K_i a_0 A \sin \theta + b_3 \omega^4 - b_1 \omega^2 - j b_2 \omega^3 \quad (39)$$

$$+ K_i a_0 A \cos \theta - j K_i a_0 A \sin \theta + b_3 \omega^4 - b_1 \omega^2 - j b_2 \omega^3 \quad (40)$$

$$+ K_i a_0 A \cos \theta - j K_i a_0 A \sin \theta + b_3 \omega^4 - b_1 \omega^2 - j b_2 \omega^3 \quad (41)$$

$$+ K_i a_0 A \cos \theta - j K_i a_0 A \sin \theta + b_3 \omega^4 - b_1 \omega^2 - j b_2 \omega^3 \quad (42)$$

$$+ K_i a_0 A \cos \theta - j K_i a_0 A \sin \theta + b_3 \omega^4 - b_1 \omega^2 - j b_2 \omega^3 \quad (43)$$

$$+ K_i a_0 A \cos \theta - j K_i a_0 A \sin \theta + b_3 \omega^4 - b_1 \omega^2 - j b_2 \omega^3 \quad (44)$$

$$+ K_i a_0 A \cos \theta - j K_i a_0 A \sin \theta + b_3 \omega^4 - b_1 \omega^2 - j b_2 \omega^3 \quad (45)$$

$$+ K_i a_0 A \cos \theta - j K_i a_0 A \sin \theta + b_3 \omega^4 - b_1 \omega^2 - j b_2 \omega^3 \quad (46)$$

$$+ K_i a_0 A \cos \theta - j K_i a_0 A \sin \theta + b_3 \omega^4 - b_1 \omega^2 - j b_2 \omega^3 \quad (47)$$

$$+ K_i a_0 A \cos \theta - j K_i a_0 A \sin \theta + b_3 \omega^4 - b_1 \omega^2 - j b_2 \omega^3 \quad (48)$$

$$+ K_i a_0 A \cos \theta - j K_i a_0 A \sin \theta + b_3 \omega^4 - b_1 \omega^2 - j b_2 \omega^3 \quad (49)$$

$$+ K_i a_0 A \cos \theta - j K_i a_0 A \sin \theta + b_3 \omega^4 - b_1 \omega^2 - j b_2 \omega^3 \quad (50)$$

Fig. 4 and Fig. 5 show the swarm positions at the first and last iterations of the optimization process. The optimum values of  $K_p$  and  $K_i$  obtained for roll axis are,

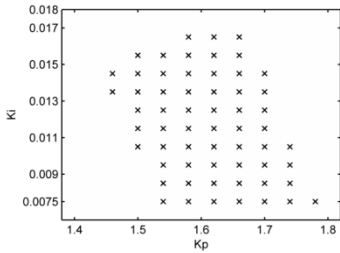
$$K_{px} = 1.59, K_{ix} = 0.0075 \quad (25)$$


Fig. 4: The swarm position at the first iteration

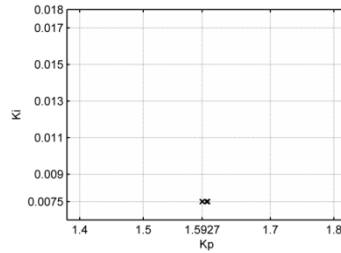


Fig. 5: The swarm position at the final iteration

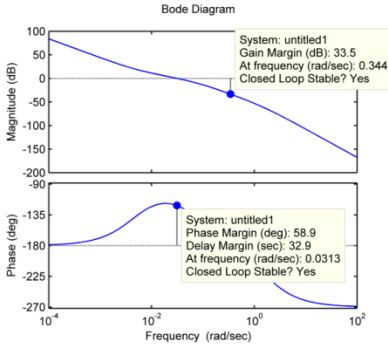


Fig. 6a: Bode plot for the Kharitonov plant  $G_{11}$ .

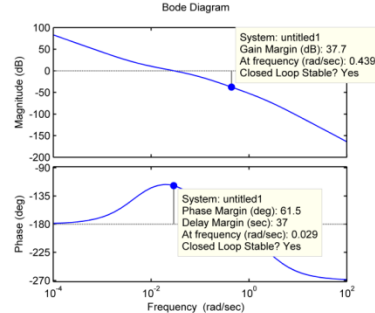


Fig. 6b: Bode plot for the Kharitonov plant  $G_{12}$ .

Similarly, the optimized PID controller values are determined for the pitch and yaw axes. The optimum  $K_p$  and  $K_i$  values for the pitch axis and yaw axis are given by Eq. 26 and Eq. 27 respectively.

$$K_{py} = 1.74, K_{iy} = 0.0076 \quad (26)$$

$$K_{pz} = 1.3, K_{iz} = 0.0074 \quad (27)$$

### 4. Simulation results and conclusion

The equation of motion for a rigid spacecraft [7] is given by,

$$J\dot{\omega} + \omega \times J\omega = T_c \quad (28)$$

The Bode plots corresponding to the Kharitonov interval plants  $G_{11}$  and  $G_{12}$  shown in Fig. 6a and Fig. 6b respectively indicate that the gain and phase margins lie within the specified intervals of [30, 38] decibels and [48.15, 65.5] degrees respectively.

$$\dot{\omega} = J^{-1}[T_c - (\omega \times J\omega)] \quad (29)$$

Simulation of the three axis attitude control system for the rigid spacecraft with uncertain parameters is carried out using the circuit shown in Fig. 7. The rigid spacecraft Simulink subsystem block shown in Fig. 8 is built using Eq. 29.

The values of  $K_p$ ,  $K_i$  and  $K_d$  before optimization are as given by Eq. 5, Eq. 13 and Eq. 14 respectively.

The step response of the uncertain spacecraft three axis attitude control system after and before optimization of the controller gains is as shown in Fig. 9 and Fig. 10 respectively.

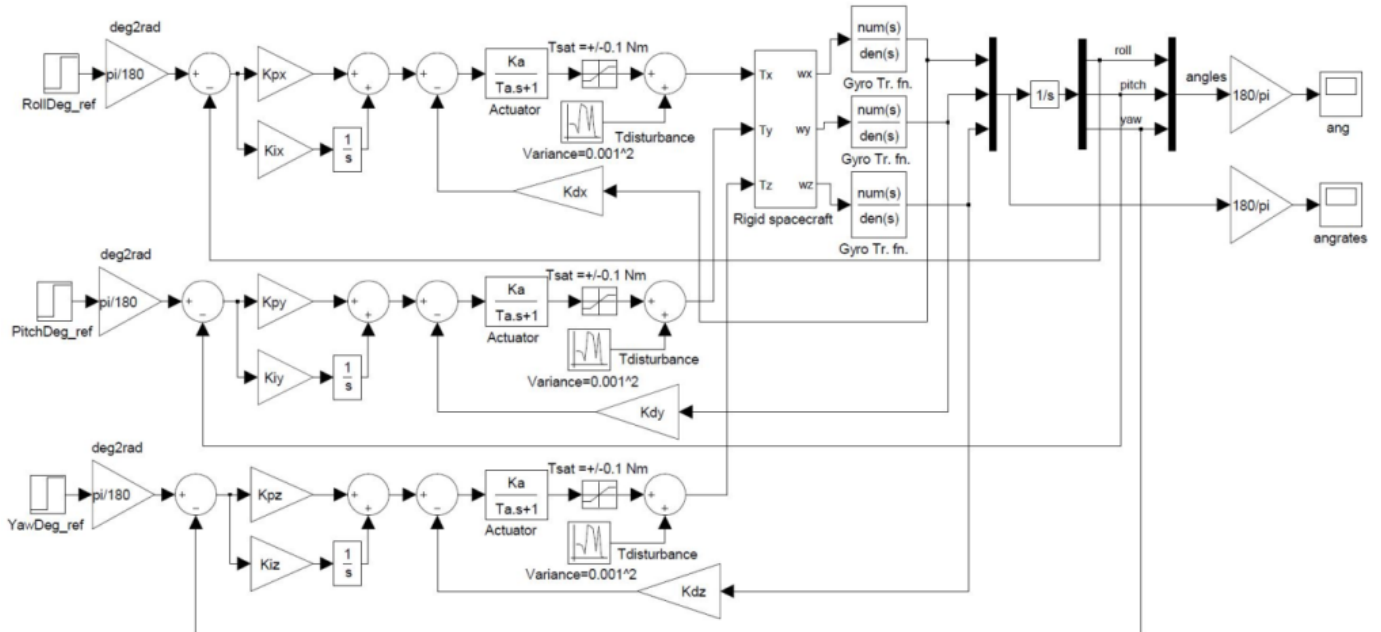


Fig.7: Rigid spacecraft three axis attitude control system



- [18] Chen Z & Huang J, "Attitude tracking and disturbance rejection of rigid spacecraft by adaptive control", *IEEE Trans. Autom. Control.*, Vol.54, No.3, (2009), pp.600-605.
- [19] Shi JF, Ulrich S & Allen A, "Spacecraft adaptive attitude control with application to space station free-flyer robotic capture", *AIAA Guidance, Navigation, and Control Conference, Kissimmee*, (2015), pp.1-23.
- [20] Sheng S & Sun C, "An adaptive attitude tracking control approach for an unmanned helicopter with parametric uncertainties and measurement noises", *Int. J. Control Autom.*, Vol.14, No.1, (2016), pp.217-228.
- [21] Zou A, de Ruiter AHJ & Kumar KD, "Finite-time attitude tracking control for rigid spacecraft with control input constraints", *IET Control Theory and Applications*, Vol.11, No.7, (2017), pp.931-940.
- [22] Li Y, Zhaowei S & Dong Y, "Time efficient robust PID plus controller for satellite attitude stabilization control considering angular velocity and control torque constraint", *Journal of Aerospace Engineering*, Vol.30, No.5, (2017).
- [23] Huang YJ & Wang YJ, "Robust PID tuning strategy for uncertain plants based on the Kharitonov theorem", *ISA Trans*, Vol.39, No.4, (2000), pp.419-431.
- [24] Eberhart R & Kennedy J, "A new optimizer using particle swarm theory", *Proceedings of the Sixth International Symposium on Micro Machine and Human Science*, (1995).
- [25] Remya S, Priya CK & Priyanka CP, "PID controller design using particle swarm optimization for servo actuation system of reusable launch vehicle", *International Journal of Advanced Research in Electrical, Electronics and Instrumentation Engineering*, Vol.4, No.8, (2015), pp.7226-7236.
- [26] Kumar A & Gupta R, "Compare the results of tuning of PID controller by using PSO and GA technique for AVR system", *Intern. J. Adv. Res. Comput. Engin. Technol.*, Vol.2, No.6, (2013), pp.2130-2138.
- [27] AL-MulaHumadi R, Abbas N & Hammadi W, "PID parameters optimization using adaptive PSO algorithm for a DCSM position control", *International Journal of Electrical Engineering and Technology*, Vol.4, No.4, (2013), pp.1-13.
- [28] Ahmadzadeh R, "Particle Swarm Optimization (Vectorized Code)". (2014).
- [29] Sarma S, Kulkarni AK, Venkateswaralu A, Natarajan P & Malik NK, "Spacecraft dynamics modeling and simulation using Matlab-Simulink", *Third National Conference on Mathematical Techniques Emerging Paradigms for Electronics and IT Industries*, (2010).